Reaction of Cr+, Mn+, Fe+, Co+, and Ni+ with O2 and N2O. Examination of the translational energy dependence of the cross sections of endothermic reactions

P. B. Armentrout, L. F. Halle, and J. L. Beauchamp

Citation: The Journal of Chemical Physics **76**, 2449 (1982); doi: 10.1063/1.443274
View online: http://dx.doi.org/10.1063/1.443274
View Table of Contents: http://scitation.aip.org/content/aip/journal/jcp/76/5?ver=pdfcov
Published by the AIP Publishing

Reaction of Cr^+, Mn^+, Fe^+, Co^+, and Ni^+ with O_2 and N_2O. Examination of the translational energy dependence of the cross sections of endothermic reactions[a)]

P. B. Armentrout[b)]

Bell Laboratories, Murray Hill, New Jersey 07974
and Arthur Amos Noyes Laboratory of Chemical Physics, California Institute of Technology, Pasadena, California 91125

L. F. Halle and J. L. Beauchamp

Arthur Amos Noyes Laboratory of Chemical Physics, California Institute of Technology, Pasadena, California 91125
(Received 24 September 1981; accepted 13 November 1981)

Reactions of Cr^+, Mn^+, Fe^+, Co^+, and Ni^+ with O_2 and N_2O to yield metal oxide ions are examined using an ion beam apparatus. Reaction cross sections σ as a function of ion translational energy E are reported. With one exception, $Fe^+ + N_2O$, the cross sections exhibit an energy threshold E_o. Several models are used to interpret the excitation functions for the O_2 reactions and it is concluded that the classical line-of-centers form $\sigma \alpha (1-E_o/E)$ is most useful. Bond energies derived in this manner are $D°(CrO^+) = 3.45 \pm 0.1$ eV, $D°(MnO^+) = 2.48 \pm 0.1$ eV, $D°(FeO^+) = 3.01 \pm 0.1$ eV, $D°(CoO^+) = 2.76 \pm 0.1$ eV, and $D°(NiO^+) = 1.95 \pm 0.1$ eV. Since these bond energies are all greater than $D°(N_2\text{–}O) = 1.7$ eV, the observation of energy thresholds for the reactions with N_2O are surprising. These results are explained in terms of a qualitative view of the electronic potential energy surfaces involved.

INTRODUCTION

The examination of gas-phase reactions of metal atoms with various oxidants has been an active area of research. Such processes are important in atmospheric chemistry[1] and often form chemiluminescent products, which may provide the basis for new laser systems. Most previous studies have been aimed primarily at this latter point and have measured reaction rates and chemiluminescence from the reactions of a variety of neutral atoms.[2–5] Few involving transition metals have been included.[3–5] Studies of the reactions of ionized metal atoms with oxidants are beginning to become available.[6–9] In the present work, we measure the kinetic energy dependent cross sections for formation of diatomic transition metal oxide ions via the reactions

$$M^+ + O_2 \rightarrow MO^+ + O \qquad (1)$$

and

$$M^+ + N_2O \rightarrow MO^+ + N_2 \ , \qquad (2)$$

where M = Cr, Mn, Fe, Co, and Ni. One of the intents of such a systematic study is to help identify trends in reactivity and bonding of transition metal systems. As such, this paper represents a continuation of previous efforts which have characterized metal hydrides,[10,11] metal alkyls,[11] and metal carbenes.[12] The thermodynamic conclusions presented here have been reported in brief form previously.[13]

Thermodynamic and spectroscopic information concerning the metal oxide ions is scarce. Tables I and II list the thermodynamic data available for the diatomic metal oxide and the metal dioxide systems. Table III gives the states of the reactant metal ions used in this study and the probable ground states for the metal oxide ions. Because of the lack of extensive information on the reaction products and intermediates, a detailed examination of the potential energy surfaces for Processes (1) and (2) is impossible. However, speculation concerning the gross features of a simple surface taken along the reaction coordinates is instructive.

For all metals, Reaction (1) should be endothermic (Table I), as is verified experimentally in this study. Since there are no obvious spin or orbital symmetry restrictions[14] and since both ground state $O_2(^3\Sigma_g^-)$ (Ref. 15) and the metal oxide ions[16] correlate adiabatically with $O(^3P)$ atoms, we expect the reactants to correlate smoothly with ground state products. Figure 1(a) shows a likely surface for both a collinear and perpendicular approach of the metal ion to the O_2 bond. The former should lead to a potential well due to the ion–molecule polarization interaction[17,18] before yielding products. The latter approach should also have a polarization potential well, but may also form a transient MO_2^+ intermediate.

The thermochemistry in Table I predicts that the reactions of N_2O with all metal ions considered here should be exothermic; however, the generalized surface for these processes is potentially much more complex than for the O_2 reactions. This is primarily because ground state $N_2O(^1\Sigma^+)$ does not correlate with ground state $N_2(^1\Sigma_g^+) + O(^3P)$, but rather with $O(^1D)$ (Ref. 19), 1.97 eV higher in energy.[20] Thermal dissociation of N_2O is observed to occur via a singlet–triplet surface crossing with an activation energy of about 2.7 eV.[21] Figure 1(b) (dashed lines) shows the N_2O sur-

[a)] Contribution No. 6493 Chem. Dept., Caltech, Pasadena, CA 91125.
[b)] Present address, Chem. Dept. U. California, Berkeley, CA 94720.

 0021-9606/82/052449-09$02.10

TABLE I. Thermochemistry of diatomic transition metal oxides.[a]

M	Ionization potential (M)[b]	$D°(MO)$	Ionization potential (MO) Literature	Ionization potential (MO) This study[c]	$D°(M^+–O)$ Literature[d]	$D°(M^+–O)$ This study
Cr	6.76	4.38 ± 0.3[e]	8.4 ± 0.5[e]	7.7 ± 0.3	2.74 ± 0.6 3.1 ± 0.8[f]	3.45 ± 0.1
Mn	7.43	3.70 ± 0.17[g]	8.6 ± 0.5[h]	8.65 ± 0.2	2.53 ± 0.6	2.48 ± 0.1
Fe	7.87	4.03 ± 0.13[i,j]	8.8 ± 0.2[i,j]	8.9 ± 0.16	3.15 ± 0.24	3.01 ± 0.1
Co	7.86	3.77 ± 0.17[k,l]	9.0 ± 0.5[k]	8.9 ± 0.2	2.63 ± 0.6	2.76 ± 0.1
Ni	7.63	3.82 ± 0.22[l,m]	9.5 ± 0.3[m]	9.5 ± 0.2	1.95 ± 0.4	1.95 ± 0.1
Al	5.98	5.26 ± 0.04[n]	9.53 ± 0.15[o]	9.46 ± 0.06	1.71 ± 0.16	1.78 ± 0.04

[a]All values in eV.
[b]Reference 20.
[c]Derived from $IP(MO) = D°(MO) - D°(MO^+) + IP(M)$.
[d]Except as noted, derived from $D°(MO^+) = D°(MO) + IP(M) - IP(MO)$.
[e]R. T. Grimley, R. P. Burns, and M. G. Inghram, J. Chem. Phys. **34**, 664 (1961).
[f]Derived from $D°(CrO^+) = D°(CrO_2) + IP(Cr) - AP(CrO^+, CrO_2)$. $D°(CrO_2)$ from Table II. $AP(CrO^+, CrO_2) = 13.5 \pm 0.5$ eV, appearance potential of CrO^+ from CrO_2. From Ref. e.
[g]C. J. Cheetam and R. F. Barrow, Adv. High Temp. Chem. **1**, 7 (1967).
[h]Estimate based on a comparison of the relative ionization potentials of M vs MO.
[i]E. Murad, J. Chem. Phys. **73**, 1381 (1980).
[j]D. L. Hildenbrand, Chem. Phys. Lett. **34**, 352 (1975).
[k]R. T. Grimley, R. P. Burns, and M. G. Inghram, J. Chem. Phys. **45**, 4158 (1966).
[l]S. Smoes, F. Mandy, A. Auwera-Mahieu, and J. Drowart, Bull. Soc. Chim. Belg. **81**, 45 (1972).
[m]R. T. Grimley, R. P. Burns, and M. G. Inghram, J. Chem. Phys. **35**, 551 (1961).
[n]J. Drowart, Faraday Symp. Chem. Soc. **8**, 165 (1974).
[o]D. L. Hildenbrand, Chem. Phys. Lett. **20**, 127 (1973).

faces schematically. How a metal ion will interact with such a complex surface is not clear *a priori*, but since the metal oxide ions do correlate with $O(^3P)$, we might expect the interaction to be centered on the N_2O surface crossing.[22] The present study reveals activation barriers for all the metal ions but Fe^+. Using an empirically determined activation barrier, we can draw a likely reaction surface. Figure 1(b) shows the result for one example, Cr^+, and includes the possibility that electronically excited MO^+ species may be formed. Unfortunately, we have no means of experimentally examining such a possibility. Also unfortunate is that most previous studies[2–5] of neutral metal atom reactions with O_2 and N_2O examine only formation of chemiluminescent products and not total reaction yields. Consequently, meaningful comparisons between the present and previous work cannot be made.

TABLE II. Thermochemistry of transition metal dioxides.[a]

M	$D°(MO_2)$[b]	Ionization potential (MO_2)	$D°(MO^+–O)$[c]
Cr	9.85 ± 0.65[d]	10.3 ± 0.5[d]	3.6 ± 1.0 2.9 ± 0.9
Fe	8.64 ± 0.22[e]	9.5 ± 0.5[e]	3.9 ± 0.6

[a]All values in eV.
[b]$D°(MO_2)$ is the energy for the process $MO_2 \rightarrow M + 2O$.
[c]Derived from $D°(MO^+–O) = D°(MO_2) - D°(MO) + IP(MO) - IP(MO_2)$. Other values required from Table I.
[d]R. T. Grimley, R. P. Burns, and M. G. Inghram, J. Chem. Phys. **34**, 664 (1961).
[e]D. L. Hildenbrand, Chem. Phys. Lett. **34**, 352 (1975).

Of additional interest is a detailed examination of the translational energy dependence of the cross sections for Reactions (1) and (2). No accepted form for this dependence presently exists, although many possibilities have been forwarded and applied to experiment.[12(a)] In many respects, the present study provides a unique opportunity to test these suggested forms. First, the reactions are simple involving only three or four atoms. Second, the reactions are examined over a broad energy

TABLE III. States of reactant metal ions and predicted ground states of metal oxide ions.

M^+[a]	MO^+[b]
$Cr^+(^6S)$	$CrO^+(^4\Pi)$
$Mn^+(^7S)$	$MnO^+(^5\Sigma^+)$ $MnO^+(^5\Pi)$
$Fe^+(^6D)$[c] $Fe^+(^4F)$	$FeO^+(^4\Delta)$
$Co^+(^3F)$	$CoO^+(^3\Sigma^-)$ $CoO^+(^3\Pi)$ $CoO^+(^3\Phi)$
$Ni^+(^2D)$	$NiO^+(^2\Pi)$ $NiO^+(^4\Sigma^-)$

[a]Reference 20.
[b]Reference 16. The first state listed is the most likely ground state.
[c]$Fe^+(^6D)$ is the ground state. $Fe^+(^4F)$ is the first excited state at 0.23 eV and may comprise up to about 20% of the iron ion beam.

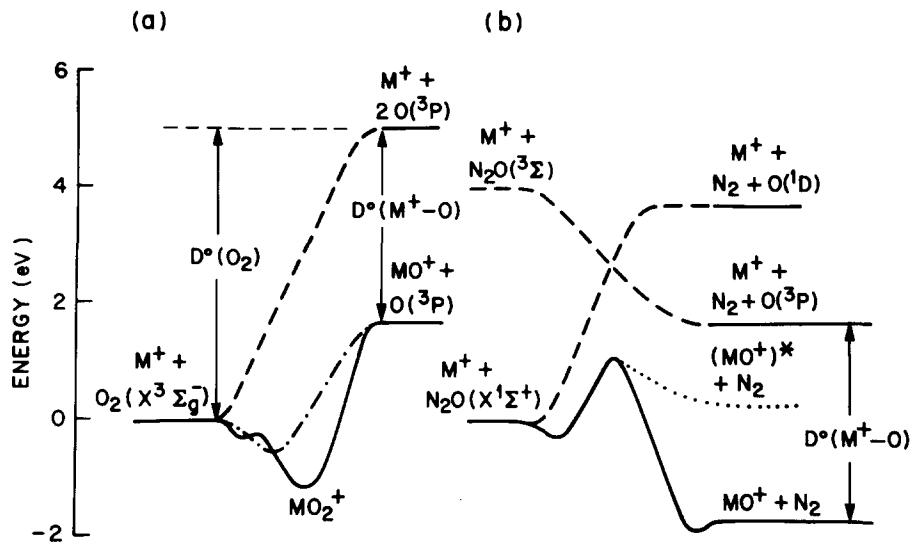

FIG. 1. Postulated reaction coordinate diagrams for Reaction (1), part a, and Reaction (2), part b. (The energies of the asymptotic states shown correspond to the $M^+ = Cr^+$ system.) Dashed lines indicate the approximate dissociative behavior of O_2 and N_2O in the absence of metal ions. Part a shows a postulated surface resulting from both a collinear (dot–dashed line) and perpendicular (full line) approach of a metal ion to O_2. In part b, the energy barrier for the $M^+ + N_2O$ reaction is that determined for Cr^+ in this study. The possibility of forming electronically excited MO^+ (arbitrarily placed on the energy scale) is indicated by the dotted line.

range. Third, as the metal ion reactant is changed, the general behavior of the cross sections is observed to remain nearly the same but the energy thresholds for reaction differ markedly. Fourth, in contrast to most previous work in our labs, thermodynamic information concerning the product ions, although sketchy, is available (Table I). Finally, at least in the case of O_2, the energy threshold for reaction E_0 is expected to equal the difference in bond dissociation energies of the bonds broken and formed during reaction; that is, the reverse of Reaction (1) has no activation barrier [Fig. 1(a)]. This is because in a reaction between ions and neutrals, the polarization interaction energy is usually sufficient to overcome activation energies. The common empirical observation that exothermic ion–molecule reactions proceed with no energy barrier attests to the validity of this conclusion. Exceptions to this rule are generally the result of spin or orbital symmetry restrictions on the reaction.[17] As discussed above, the reactions of metal ions with N_2O appear to be a class of such exceptions.

EXPERIMENTAL

Apparatus

The apparatus and experimental techniques have been detailed previously.[12(a)] Briefly, metal ions are extracted from a surface ionization source, accelerated, momentum analyzed, decelerated to the desired interaction energy, and focused into a collision chamber filled with O_2 or N_2O. Pressures of the reactant gas are kept sufficiently low [$(1-5)\times10^{-3}$ Torr], such that only single collision events need be considered. Unreacted metal ions and product metal oxide ions exiting the chamber are collected and detected using a quadrupole mass filter and Channeltron electron multiplier operated in a pulse counting mode. Signal intensities are corrected for the mass discrimination of the mass filter.

Reaction cross sections are calculated from

$$I_p = (I_p + I_0)\exp(-n\sigma l)\,, \qquad (3)$$

where I_0 and I_p are the transmitted reactant and product ion beam intensities, respectively, n is the number density of the target gas, and l is the length of the interaction region (~5 mm). The greatest uncertainty in these measurements is the ion detection efficiency. We estimate, however, that the cross sections reported are accurate to within a factor of 2.

The metal ion source, previously described,[10] utilizes vaporization and surface ionization of metal halide salts: here, the hydrated forms of $CrCl_3$, $MnCl_2$, $FeCl_3$, $CoCl_2$, and $NiCl_2$. The surface ionization method of producing metal ions minimizes the formation of excited metal ion states. At the filament temperature used (~2500 K), calculations show that >98% of the Cr^+, Mn^+, and Ni^+ ions should be in their ground state manifolds ^6S, ^7S, and ^2D, respectively. Fe^+ and Co^+ may have a maximum population of about 20% in their first excited state manifolds, $Fe^+(^4F)$ at 0.23 eV and $Co^+(^5F)$ at 0.43 eV,[20] with the remainder in their respective ground states ^6D and ^3F. In order to observe the effects of excited species, their lifetime must exceed about 10 μS, the approximate flight time of the ions. Attenuation experiments[23] reveal only a single electronic state in all cases suggesting excited states are absent. However, this assumes that different states have substantially different cross sections for interaction with the attenuating gases. Extensive studies[11,12,24] involving Co^+ in our laboratories have indicated no excited state population.

The energy of the ion beam is taken nominally as the difference in potential between the collision chamber and the center of the surface ionization filament, the latter being determined by a resistive divider. This energy is verified by use of a retarding field energy analyzer.[12(a)] Agreement was always within 0.3 eV. This potential systematic error in the energy scale is not included in the bond energies derived in this study. The nominal reaction energy E has a distribution determined by the spread in the ion beam energy (~0.7 eV in the laboratory frame) and the thermal motion of the reactant gas.

This latter effect is generally the more important, having a width (center-of-mass frame) of $(11.1\ \gamma kTE)^{1/2}$, where $\gamma = m/(m+M)$, m and M being the masses of the incident particle and target gas, and T is the temperature of the reactant gas (~300 K).[25] Chantry[25] has shown that for a linear cross section this displaces the apparent threshold to lower energies by $3\gamma kT$ (~0.05 eV, center-of-mass frame, in the present experiments). In the Appendix, it is shown that for a line-of-centers cross section this displacement is $\frac{1}{2}\gamma kT$ (~0.01 eV, center-of-mass frame, in the present experiments). For simplicity, these effects will be ignored in the comparison of various cross section forms. However, the final fits to the data include this effect explicitly by convoluting the proposed form for the cross section with the energy distribution. The Appendix derives an analytic formula for the convoluted cross section in the case of the line-of-centers model.

INTERPRETATION OF EXPERIMENTS

Threshold region

In order to accurately interpret experiments such as these, we require the energy dependence of the true microscopic reaction cross section $\sigma(E)$. It has been shown that direct deconvolution of the phenomonological cross section does not yield a unique cross section independent of experimental energy distributions.[26] Instead, a choice for $\sigma(E)$ is made and shown to reproduce the data after convolution with the experimental conditions.[12(a)] A common general form for $\sigma(E)$ is

$$\sigma(E) = \sigma_0(E - E_0)^n/E^m , \tag{4}$$

where σ_0 is an energy independent cross section, E is the total energy, E_0 is the reaction threshold, and n and m are variable parameters implicitly or explicitly assumed to be related to the degrees of freedom of the reactants, products, or reaction intermediates. We assume here that E is equivalent to the ion kinetic energy and neglect any internal energy of the reactants.

Specific examples of Eq. (4) considered below are a linear form ($n=1$ and $m=0$), a form derived by Eu and Liu[27] from scattering theory ($n=m=1/2$), the classical line-of-centers model ($n=m=1$),[28] and a form found useful in a previous study ($n=m=2$).[8] For these four forms, a plot of $(\sigma E^m)^{1/n}$ vs E, utilizing the experimental cross sections, is linear with an intercept of E_0 and a slope of $\sigma_0^{1/n}$. A linear least squares analysis provides the values of σ_0, E_0, and the error in E_0 (one standard deviation) cited below.

Also examined is a form similar to the line-of-centers but derived from a sequential impulse scattering model for endothermic atom–diatom reactions.[10(a)] This model predicts $n=m=1$ but replaces E_0 with an effective threshold

$$E_1 = E_0/(4\cos^2\beta\sin^2\beta) , \tag{5}$$

where $\cos^2\beta = AC/(A+B)(B+C)$ and A, B, C are the masses of the incident particle, the atom transferred during reaction, and the neutral product, respectively. The mass factor in the denominator of Eq. (5) is well known as the fraction of energy transferred from translation to vibration for a collinear atom–diatom collision in the limit of a loose oscillator.[28] For this form of the cross section, the endothermicity E_0 is found from the experimental data by applying this mass factor to the value of E_0 found for the line-of-centers form; that is, E_0 (line-of-centers) $= E_1$.

More general examples of Eq. (4) considered below are formulas where n is undetermined but m is taken as 0, 1, and n. In these cases, E_0 is taken from literature data and a linear least squares analysis of a plot of $\log(\sigma E^m)$ vs $\log(E-E_0)$ yields n as the slope with the errors in n taken as one standard deviation.

High energy region

As the ion energy is increased in the present experiments, the probability of forming product ions with sufficient internal energy to dissociate before detection increases. The threshold for such a process is simply the bond dissociation energy of the reactant neutral

$$M^+ + XO \rightarrow [MO^+]^* + X \rightarrow M^+ + O + X , \tag{6}$$

where X = O or N_2 and the asterisk indicates an internally excited species. Such a process can greatly affect the experimentally observed cross section for formation of MO^+. Indeed, the cross section typically reaches a maximum near the reactant neutral bond energy. If the neutral product is atomic (X = O), the cross section then falls rapidly, since any internal energy is located in the diatomic ionic product. If the neutral product is polyatomic ($X = N_2$) the cross section decreases more gradually, since some internal energy now resides in this product.

We can model the high energy behavior for atom–diatom reactions using the sequential impulse scattering model mentioned above.[10(a)] It has proven useful in understanding a number of endothermic atom–diatom reaction cross sections.[10–13] Unfortunately, the model is inapplicable to processes such as Reaction (2). In these cases, the high energy behavior is treated on an empirical basis.

RESULTS

Reactions with O_2

Cross sections for Reactions (1) as a function of relative kinetic energy are shown in Figs. 2 and 3 for $M^+ = Cr^+$, Mn^+, Fe^+, Co^+, and Ni^+. The cross sections rise from apparent thresholds of between 1 and 3 eV and peak at 5–6 eV, in good agreement with $D^\circ_{298}(O_2) = 5.16$ eV.[29] The small shoulder near threshold in the Fe^+ data may be due to the reactions of a small percentage of excited states. It is believed that the cross sections are nonzero at the lowest energies because reactions occur outside the collision chamber where the ion beam has higher kinetic energies. While not obvious from these figures (but apparent from a plot of $\log\sigma$ vs $\log E$), all the experimental cross sections decrease as $E^{-2.1\pm0.1}$ at energies immediately above the peak and as $E^{-6\pm0.5}$ at energies beginning about 10 eV.

As discussed in the previous section, the threshold

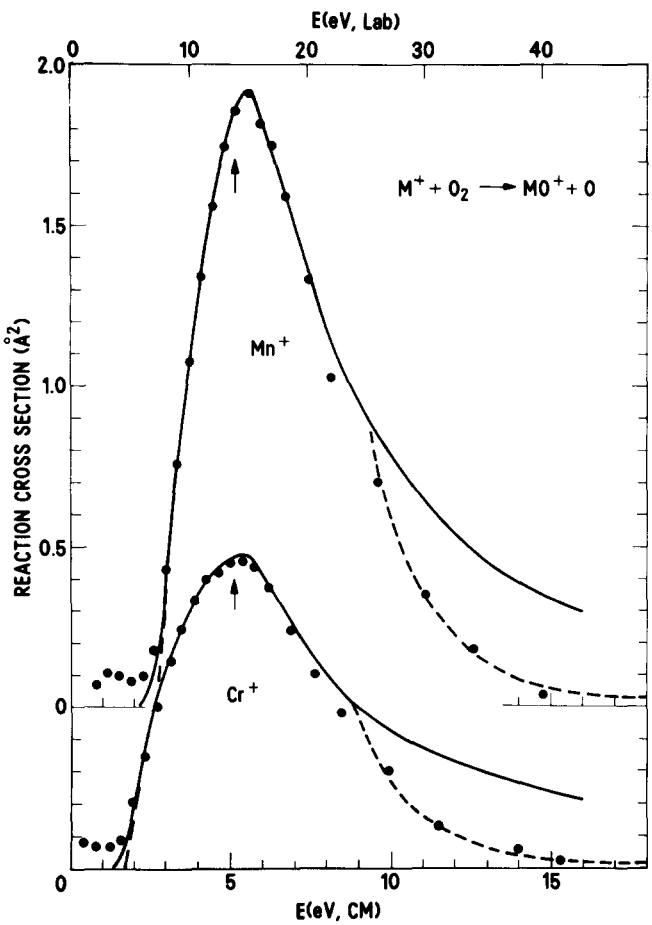

FIG. 2. Variation in cross section for the reaction of Mn^+ and Cr^+ with O_2 as a function of kinetic energy in the center-of-mass frame (lower scale) and laboratory scale (upper frame, Mn^+ reaction). The vertical scales for the two reactions are offset by 0.5 Å². Below the bond energy of O_2 at 5.16 eV (indicated by arrows), the lines are fits to the data using the line-of-centers model with threshold energies of 1.71 eV for Cr^+ and 2.68 eV for Mn^+. The full lines indicate the model as convoluted with the experimental energy distribution while the long dashed lines are unconvoluted. At higher energies, the lines are fits described in the text.

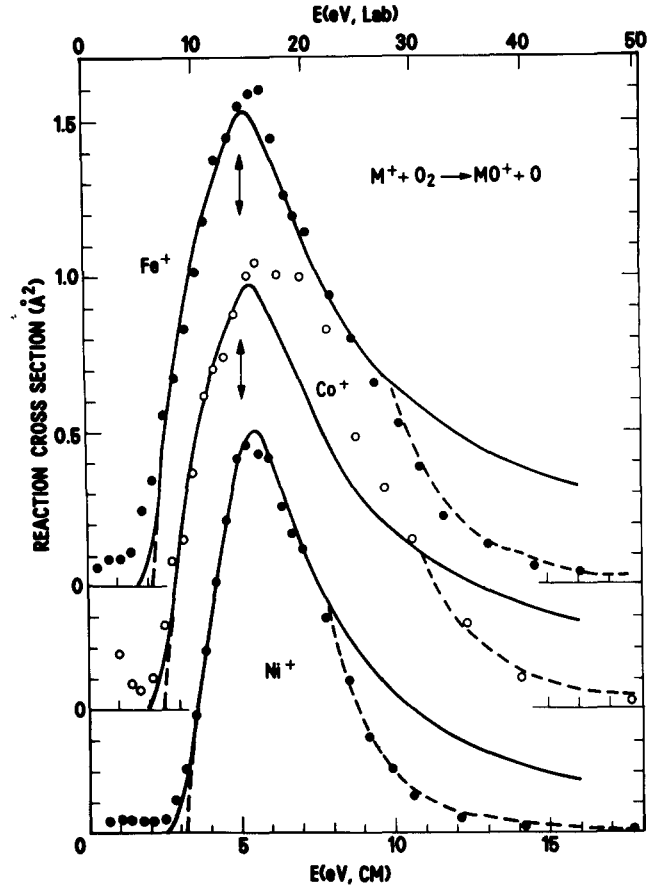

FIG. 3. Variation in cross section for the reaction of Fe^+, Co^+, and Ni^+, with O_2 as a function of kinetic energy in the center-of-mass frame (lower scale) and laboratory scale (upper scale, Ni^+ reaction). The vertical scales for the reactions are offset by 0.4 Å² each. Below the bond energy of O_2 at 5.16 eV (indicated by arrows), the lines are fits to the data using the line-of-centers model with threshold energies of 2.15 eV for Fe^+, 2.40 eV for Co^+, and 3.21 eV for Ni^+. The full lines indicate the model as convoluted with the experimental energy distribution while the long dashed lines are unconvoluted. At higher energies, the lines are fits described in the text.

regions of these cross sections may be modeled using several variations of Eq. (4). Using the analysis presented above, the values of n and E_0 listed in Tables IV and V, respectively, are derived from the O_2 data. It should be noted that the Eu and Liu form $\sigma_0(1 - E_0/E)^{1/2}$, cannot reproduce the data near threshold even if convoluted by the experimental energy distributions. The linear form $\sigma_0(E - E_0)$ is successful over a limited range. All other forms reproduce the data up to the peak reasonably well.

Included in this analysis, Tables IV and V, are the results of Rutherford and Vroom[7] for the reaction

$$Al^+ + O_2 \rightarrow AlO^+ + O \ . \qquad (7)$$

The only substantive difference between their experimental technique and ours was the use of a crossed beam geometry rather than the beam-gas approach

TABLE IV. Values of n for Reaction (1): $M^+ + O_2 \rightarrow MO^+ + O$.

Cross section form	Metal Ion Reactant Cr	Mn	Fe	Co	Ni	Al	Avg
$(E - E_0)^n$	0.4 ± 0.3	0.7 ± 0.2	0.7 ± 0.1	0.6 ± 0.2	0.8 ± 0.2	0.8 ± 0.2	0.7 ± 0.2
$(E - E_0)^n/E$	0.7 ± 0.3	1.0 ± 0.4	1.2 ± 0.1	0.9 ± 0.4	1.1 ± 0.3	0.94 ± 0.4	0.97 ± 0.17
$(1 - E_0/E)^n$	0.6 ± 0.5	1.0 ± 0.4	1.3 ± 0.2	0.9 ± 0.4	1.1 ± 0.4	0.9 ± 0.3	0.97 ± 0.23

TABLE V. Values of E_0 for Reactions (1): $M^+ + O_2 \rightarrow MO^+ + O$.

Cross section form	Metal Ion Reactant Cr	Mn	Fe	Co	Ni	Al
$(E-E_0)$	1.35	2.38	1.29	1.92	2.92	3.34
$(1-E_0/E)^{1/2}$	2.28	3.25	2.93	3.10	3.65	3.67
$(1-E_0/E)$	1.71	2.68	2.15	2.40	3.21	3.38
$(1-E_1/E)$	1.62	2.54	2.04	2.29	3.06	2.91
$(1-E_0/E)^2$	1.30	2.12	1.44	1.73	2.61	3.10
Literature[a] E_0	2.42 ± 0.6	2.63	2.01	2.53	3.21	3.45
	2.1 ± 0.8	± 0.6	± 0.24	± 0.6	± 0.4	± 0.16

[a]Calculated from $D^\circ(O_2) - D^\circ(M^+ - O)$ with $D^\circ(O_2) = 5.16$ eV (Ref. 29) and $D^\circ(M^+ - O)$ from Table I.

used here. This markedly narrows the kinetic energy distribution and leads to a more sharply defined reaction threshold. Their results, shown in Fig. 4, behave similarly to the present results, peaking at 5–6 eV, decreasing first as $E^{-1.7}$ and then as $E^{-6.5}$ beginning at 25 eV.

We conclude that the line-of-centers model yields the best thermochemical results. This is seen by the fact that the proposed general models $(E-E_0)^n/E$ and $(1-E_0/E)^n$ both yield an average value for n of approximately 1.0 (Table IV). This is further substantiated by the very good agreement between the threshold energy predicted from the literature value for the Al^+ reaction and that yielded by the line-of-centers model (Table V). This agreement is particularly significant, since for this reaction the experimental energy distribution is minimized and the value for $D^\circ(Al^+-O)$ is well established.

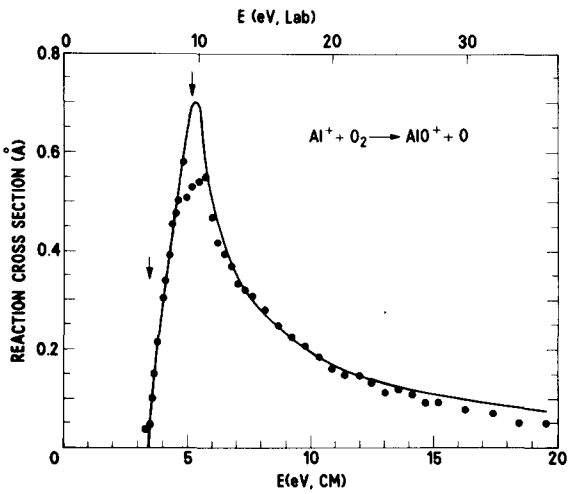

FIG. 4. Variation in cross section for the reaction of Al^+ with O_2 as a function of kinetic energy in the center-of-mass frame (lower scale) and laboratory scale (upper scale). The data are from Rutherford and Vroom (Ref. 7). The arrows indicate the bond dissociation energy of O_2 (5.16 eV) and the threshold energy (3.45 ± 0.16 eV) predicted by the difference between the O_2 and AlO^+ bond energies. The line is a fit to the data using the line-of-centers model with a threshold energy of 3.38 eV and the similar sequential impulse model as described in the text.

The line-of-centers model also does a good job of describing the energy dependence of the reaction cross sections in the threshold region. This is illustrated in Figs. 2, 3, and 4, where the full lines drawn are fits to the data, using the line-of-centers model convoluted with the experimental energy distribution (long dashed lines at low energy indicate the unconvoluted fit). At higher energies, the sequential impulse scattering model is used (the line-of-centers model and the sequential impulse model are identical at energies below the onset of product dissociation).[10] The fits shown use the threshold energies listed in Table V and the following values of σ_0: $Cr^+ - 1.47$ Å^2, $Mn^+ - 3.95$ Å^2, $Fe^+ - 2.63$ Å^2, $Co^+ - 2.55$ Å^2, $Ni^+ - 3.42$ Å^2, and $Al^+ - 2.0$ Å^2.[30] The model adequately describes the behavior of the data until the beginning of the E^{-6} falloff. This decrease is quite close to that predicted by Bates *et al.*,[31] $E^{-5.5}$ for energies above about 100 eV (laboratory). The falloff is empirically included in Figs. 2 and 3 (short dashed lines). For simplicity, we do not convolute the experimental energy distribution into the resultant curve at high energies. However, such a convolution would smooth the sharp break and provide a better fit to the data.

Reactions with N_2O

Cross sections for Reaction (2) as a function of relative kinetic energy are shown in Figs. 5 and 6 for $M^+ = Cr^+$, Mn^+, Fe^+, Co^+, and Ni^+. Only the reaction of the iron ion exhibits no activation energy and it has a small cross section (~1/10 that predicted by the Langevin–Gioumousis–Stevenson model[32] for ion–molecule reactions). All the cross sections decrease as $E^{-0.5\pm0.5}$ at intermediate energies and as E^{-3} beginning about 6 eV. The results of Rutherford and Vroom[7] for Reaction (2) with M = Al are in good qualitative accord with the present experiments. Their spectrum shows a threshold, peaks at 1.7 eV, decreases as $E^{-0.5}$ and then as $E^{-1.5}$ at higher energies.

It is unclear whether an interpretation of these data such as performed for Reaction (1) is warranted given the complex potential energy surface. However, to get a rough idea of the relative activation energies involved, the line-of-centers model is used to yield the results in Table VI. The model does a satisfactory job of de-

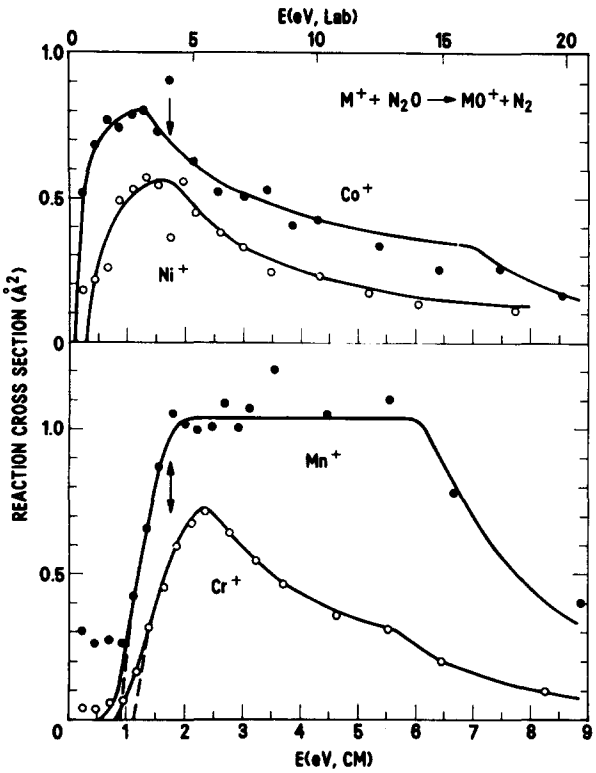

FIG. 5. Variation in cross section for the reaction of Co^+, Ni^+, Mn^+, and Cr^+, with N_2O as a function of kinetic energy in the center-of-mass frame (lower scales) and laboratory frame (upper scale, Ni^+ reaction). Below the bond energy of N_2O at 1.7 eV (indicated by arrows), the lines are fits to the data using the line-of-centers model with threshold energies as listed in Table VI. Fits at higher energies are empirically determined lines (see the text).

scribing the energy dependence of the cross sections until about $D°(N_2-O) = 1.7$ eV,[29] Fig. 5. The lines drawn at higher energies in Figs. 5 and 6 are empirical fits to the data with the intermediate energy dependence as follows: $Cr^+ - E^{-1}$; $Mn^+ - E^0$; Fe^+, Co^+, and $Ni^+ - E^{-0.5}$.

Based on the metal oxide ion thermochemistry in Table I, Reactions (2) are known to be exothermic. The origin of the activation energies observed can be explained qualitatively by noting the singlet–triplet surface crossing in the N_2O potential energy curves, as discussed in the introduction. This general explanation, however, fails to account for the relative magnitudes of the energy barriers observed (Table VI). One simple explanation for the substantially higher values of E_0 for reaction of Cr^+ and Mn^+ is that formation of ground state MO^+ is spin forbidden. Reaction of Co^+ and Ni^+ with N_2O, however, may proceed on a single potential energy surface to ground state products. If spin is indeed conserved in Reactions (2), then reaction of Fe^+ should occur predominantly with the ^4F excited state, a possible minor constituent of the iron ion beam. This could explain why the cross section for this reaction is anomalously low for an exothermic ion–molecule reaction exhibiting no activation barrier. However, attenuation measurements for Fe^+ in N_2O do not indicate the presence of more than one metal ion state.

TABLE VI. Values of E_0 and σ_0 used to fit the data for Reactions (2): $M^+ + N_2O \rightarrow MO^+ + N_2$.

M	E_0 (eV)	σ_0 (Å²)
Cr	1.1	1.47
Mn	0.9	2.05
Fe	< 0	
Co	0.09	0.87
Ni	0.3	0.71
Al	0.65	1.15

DISCUSSION

Reactions of metal ions with O_2 can be understood using the simple line-of-centers model. This model provides a reliable interpretation of the threshold regions of the cross sections for Reactions (1). This is consistent with our successful application of this model to the reactions

$$M^+ + H_2 \rightarrow MH^+ + H\,, \tag{8}$$

where M = Ba,[10(a)] Ni,[10(b)] Co,[11] Cr,[12(b)] Mn, and Fe.[33] Several neutral reactions, $K + HCl \rightarrow KCl + H$,[34] $Hg + I_2 \rightarrow HgI + I$,[35] and $Sr + HF \rightarrow SrF + H$,[36] for which the cross sections as a function of translational energy have been measured, also behave as predicted by the line-of-centers model when the reaction endothermicity is used

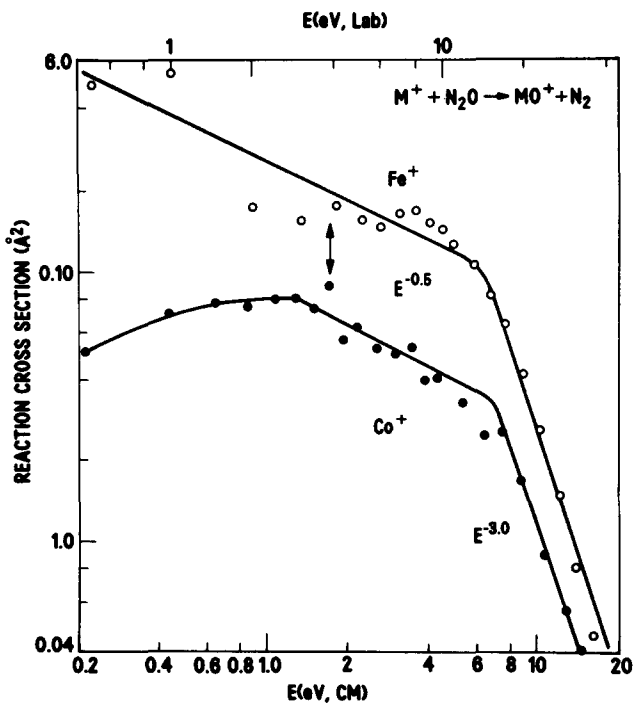

FIG. 6. Variation in cross section for the reaction of Co^+ and Fe^+, with N_2O as a function of kinetic energy in the center-of-mass frame (lower scale) and laboratory frame (upper scale, Fe^+ reaction). The data and the line for Co^+ are the same as displayed in Fig. 4. The lines through the Fe^+ data are empirically determined and have the indicated slopes. The arrows indicate the bond energy of N_2O at 1.7 eV.

as the value of E_0. This suggests that the line-of-centers model is a most useful form for describing the translational energy dependence of the cross sections for endothermic atom–diatom reactions.

Using the line-of-centers model to interpret our results for Reactions (1), the metal oxide ion bond energies and metal oxide ionization potentials listed in Table I are determined. It may be noted that these results are in sharp disagreement with the conclusions of Kappes and Staley[9,37] who studied Reactions (1) and (2) and others using ion cyclotron resonance mass spectrometry. While their experimental results generally agree with ours, they erroneously concluded that if Reactions (2) were not observed at thermal energies, then the reactions must be overall endothermic, that is, $D^\circ(M^+–O) < D^\circ(N_2–O) = 1.7$ eV. For many reactions, this would be a valid assumption; however, as discussed above, the complex nature of the N_2O potential energy curves leads to activation energies as measured in this study. The one experimental discrepancy noted is that Kappes and Staley observed both Fe^+ and Cr^+ to react slowly with N_2O. In light of the present results, this suggests that excited states of Cr^+ were present in their experiment.

It is interesting to examine the differences in the bond dissociation energies for MO^+ and MO (Table I). Both are seen to decrease as the d shell is filled. With the exception of Ni, the ionic species all have weaker bonds by about 1.0 eV. Valence bond considerations[16] predict that ionization of MO in all cases is by removal of a metal 4s electron. If the MO bond is of an ionic nature, as seems likely,[38] a weaker bond in the MO^+ species is expected since M^+ is less able to donate electrons to the oxygen atom than is M. Since the 4s electron in NiO is bonding, while in CrO, MnO, and FeO it is nonbonding,[16] the difference in ionic and neutral bond energies for NiO is substantially greater than for the other metals. While CoO is predicted to be an intermediate case,[16] the present results imply that its bonding is more like FeO than NiO.

ACKNOWLEDGMENTS

The authors would like to thank J. A. Rutherford for providing his data in tabular form. One of us (PBA) would like to thank R. A. Gottscho and J. C. Tully for heplful conversations.

APPENDIX

In this section, we derive an analytical form for the line-of-centers cross section as convoluted by the thermal motion of the target gas molecules. We use the same approach as Chantry,[25] and thus do not consider the kinetic energy distribution of the projectile ion beam. The reader is referred to the treatment of Lifschitz *et al.*[39] concerning this factor. Table A defines the symbols used in this appendix.

Chantry shows that if we deal with a monoenergetic beam interacting with molecules having an isotropic Maxwellian velocity distribution and consider E and $E_N > kT$, the energy distribution is given by

TABLE A. List of symbols.

E:	Center-of-mass energy
E_N:	Nominal c.m. energy of projectile particle, i.e., c.m. energy when $T = 0$
E_0:	Threshold energy in c.m. system
m:	Mass of projectile particle
M:	Mass of target molecule
T:	Temperature of target gas
$W_{1/2}$:	FWHM of c.m. energy distribution
γ:	$= m/(m+M)$
ϵ	$= E/\gamma kT$, dimensionless energy variable.
ϵ_N	$= E_N/\gamma kT$
ϵ_0	$= E_0/\gamma kT$

$$f(\epsilon_N, \epsilon)\, d\epsilon = (1/4\pi\epsilon_N)^{1/2} \exp[-(\epsilon^{1/2} - \epsilon_N^{1/2})^2]\, d\epsilon. \quad \text{(A1)}$$

This distribution peaks at $\epsilon = \epsilon_N$ and has a full width at half maximum (FWHM) of

$$W_{1/2} = (11.1 \gamma kT E_N)^{1/2}\ . \quad \text{(A2)}$$

The effective cross section is then given by

$$\sigma_{\text{eff}} = \int_0^\infty (\epsilon/\epsilon_N)^{1/2} \sigma(\epsilon) f(\epsilon_N, \epsilon)\, d\epsilon\ , \quad \text{(A3)}$$

where the factor $(\epsilon/\epsilon_N)^{1/2}$ is proportional to the effective interaction length.

If we consider the line-of-center form for the cross section, then for $E < E_0$, $\sigma(\epsilon) = 0$ and $E > E_0$

$$\sigma(\epsilon) = \sigma_0(1 - E_0/E) = \sigma_0(1 - \epsilon_0/\epsilon)\ , \quad \text{(A4)}$$

where σ_0 is an energy independent parameter. Substituting Eqs. (A4) and (A1) into Eq. (A3) we find

$$\sigma_{\text{eff}} = \sigma_0(4\pi\epsilon_N)^{-1/2} \int_{\epsilon_0}^\infty (1 - \epsilon_0/\epsilon) \exp[-(\epsilon^{1/2} - \epsilon_N^{1/2})^2]\, d\epsilon. \quad \text{(A5)}$$

Using the substitution $\alpha = \epsilon^{1/2} - \epsilon_N^{1/2}$, Eq. (A5) is integrated to yield

$$\sigma_{\text{eff}} = \sigma_0(4\pi\epsilon_N)^{-1/2}[1 + (\epsilon_0/\epsilon_N)^{1/2}] \exp[-(\epsilon_0^{1/2} - \epsilon_N^{1/2})^2] + (\sigma_0/2)[1 - \underline{(\epsilon_0/\epsilon_N)} + (2\epsilon_N)^{-1}][1 - \text{erf}(\epsilon_0^{1/2} - \epsilon_N^{1/2})]\ , \quad \text{(A6)}$$

where

$$\text{erf}(x) = (2/\pi^{1/2}) \int_0^x \exp(-x^2)\, dx\ ,$$

and

$$\text{erf}(-x) = -\text{erf}(x)$$

is the error function, available in tabulated form. This result is identical to that obtained by Chantry for a step-function cross section except for the ϵ_0/ϵ_N term underlined in Eq. (A6).

At energies well above threshold $\epsilon_n \gg \epsilon_0$ the first term in Eq. (A6) goes to zero, while the error function becomes equal to -1, leaving

$$\sigma_{\text{eff}} = \sigma_0[1 - (\epsilon_0/\epsilon_N) + (2\epsilon_N)^{-1}]\ . \quad \text{(A7)}$$

If we now plot $\sigma_{\text{eff}}\, \epsilon_N$ vs ϵ_N, our procedure for finding σ_0

and E_0 from the experimental data, we obtain an energy axis intercept of $\epsilon_0 - 1/2$ or $E_0 - \gamma kT/2$. Thus, a plot of σE vs E, using experimental data, should be linear at higher energies but extrapolates to an apparent threshold which is too low by $\gamma kT/2$.

[1]E. Murad, J. Geophys. Res. **83**, 5525 (1978); E. E. Ferguson and F. C. Fehsenfeld *ibid.* **73**, 6215 (1968).

[2]See, for example, R.W. Field, C. R. Jones, and H. P. Broida, J. Chem. Phys. **60**, 4377 (1974); P. J. Dagdigian, H. W. Cruse, A. Schultz, and R. N. Zare, *ibid.* **61**, 4450 (1974); R. W. Field, *Molecular Spectroscopy* (Academic, New York, 1976), Vol. II, p. 261; D. J. Eckstrom, S. A. Edelstein, D. L. Huestis, B. E. Perry, and S. W. Benson, J. Chem. Phys. **63**, 3828 (1975); W. Felder. R. K. Gould, and A. Fontijn, *ibid.* **66**, 3256 (1977); M. H. Alexander and P. J. Dagdigian, Chem. Phys. **33**, 13 (1978); J. R. Wiesenfeld and M. J. Yuen, Chem. Phys. Lett. **42**, 293 (1976); A. Fontijn and W. Felder, *Reactive Intermediates in the Gas Phase*, edited by D. W. Setser (Academic, New York, 1979), p. 59.

[3]J. B. West and H. P. Broida, J. Chem. Phys. **62**, 2566 (1975); C. Linton and H. P. Broida, J. Mol. Spectrosc. **64**, 382 (1977).

[4]L. H. Dubois and J. L. Gole, J. Chem. Phys. **66**, 779 (1977); R. W. Jones and J. L. Gole, *ibid.* **65**, 3800 (1976); C. L. Chalek and J. L. Gole, Chem. Phys. **19**, 59 (1977).

[5]J. M. Parson, L. C. Geiger, and T. J. Conway, J. Chem. Phys. **74**, 5595 (1981).

[6]R. Johnsen, H. L. Brown, and M. A. Biondi, J. Chem. Phys. **55**, 186 (1971); R. Johnsen and M. A. Biondi, *ibid.* **57**, 1975 (1972); R. Johnsen, F. R. Castell, and M. A. Biondi, *ibid.* **61**, 5404 (1974).

[7]J. A. Rutherford and D. A. Vroom, J. Chem. Phys. **65**, 4445 (1976).

[8]P. B. Armentrout and J. L. Beauchamp, Chem. Phys. **50**, 27 (1980).

[9]M. M. Kappes and R. H. Staley, J. Phys. Chem. **85**, 942 (1981).

[10](a) P. B. Armentrout and J. L. Beauchamp, Chem. Phys. **48**, 315 (1980); (b) **50**, 37 (1980).

[11]P. B. Armentrout and J. L. Beauchamp, J. Am. Chem. Soc. **102**, 1736 (1980); **103**, 784 (1981).

[12](a) P. B. Armentrout and J. L. Beauchamp, J. Chem. Phys. **74**, 2819 (1981); (b) L. F. Halle, P. B. Armentrout, and J. L. Beauchamp, J. Am. Chem. Soc. **103**, 962 (1981).

[13]P. B. Armentrout, L. F. Halle, and J. L. Beauchamp, J. Am. Chem. Soc. **103**, 6501 (1981).

[14]K. E. Shuler, J. Chem. Phys. **21**, 624 (1953).

[15]G. Herzberg, *Electronic Spectra of Polyatomic Molecules* (Van Nostrand, New York, 1966).

[16](a) S. P. Walch, Ph.D. thesis, California Institute of Technology (1977); (b) S. P. Walch and W. A. Goddard, J. Am. Chem. Soc. **100**, 1338 (1978).

[17]See, for example. V. L. Talrose, P. S. Vinogradov, and I. K. Larin, *Gas Phase Ion Chemistry*, edited by M. T. Bowers (Academic, New York, 1979), Vol. 1, p. 305.

[18]The potential well due to the ion–molecule polarization interaction should be about twice as deep for collinear approach as for perpendicular approach, since the polarizability of O_2 along its axis is about twice that of the other two axes, *Landolt–Bornstein Zahlenwerte und Fuctionen* (Springer, Berlin, 1951), Vol. 1, Part 3, p. 510, as cited in J. Applequist, J. R. Carl, and K. Fung, J. Am. Chem. Soc. **94**, 2952 (1972).

[19]G. Herzberg, *Spectra of Diatomic Molecules* (Van Nostrand, New York, 1950).

[20]C. E. Moore, Natl. Stand. Ref. Data Ser. Natl. Bur. Stand. **34** (1970).

[21]V. J. Troe and H. G. Wagner, Ber. Bunsenges. Phys. Chem. **71**, 946 (1967); A. J. Lorquet, J. C. Lorquet, and W. Forst, Chem. Phys. **51**, 253 (1980).

[22]Similar suggestions have been made previously. See, for example, J. R. Wiesenfeld and M. J. Yuen, Chem. Phys. Lett. **42**, 293 (1976).

[23]B. R. Turner, J. A. Rutherford, and D. M. J. Compton, J. Chem. Phys. **48**, 1602 (1968).

[24]P. B. Armentrout and J. L. Beauchamp, J. Am. Chem. Soc. **103**, 6628 (1981); P. B. Armetrout, L. F. Halle, and J. L. Beauchamp, *ibid.* 6624 (1981).

[25]P. J. Chantry, J. Chem. Phys. **55**, 2746 (1971).

[26]L. A. Melton and R. G. Gordon, J. Chem. Phys. **51**, 5449 (1969).

[27]B. C. Eu and W. S. Liu, J. Chem. Phys. **63**, 592 (1975).

[28]R. D. Levine and R. B. Bernstein, *Molecular Reaction Dynamics* (Oxford, New York, 1974).

[29]D. D. Wagman, W. H. Evans, V. B. Parker, I. Halow, S. M. Bailey, and R. H. Schumm, NBS Tech. Note 270-3 U.S. Government Printing Office, Washington, DC, 1968).

[30]It should be noted that the sequential impulse model includes both a two collision sequence and a one collision sequence (or stripping-like event). The fits shown in Figs. 2–4 do not include any of the latter type of event. This suggests that Reaction (1) probably proceed via a potential energy well corresponding to MO_2^+.

[31]D. R. Bates, C. J. Cook, and F. J. Smith, Proc. Phys. Soc. London **83**, 49 (1964).

[32]G. Gioumousis and D. P. Stevenson, J. Chem. Phys. **29**, 294 (1958).

[33]L. F. Halle, P. B. Armentrout, and J. L. Beauchamp (unpublished results).

[34]J. G. Pruett, F. R. Grabiner, and P. R. Brooks, J. Chem. Phys. **63**, 1173 (1975).

[35]T. M. Mayer, B. E. Wilcomb, and R. B. Bernstein, J. Chem. Phys. **67**, 3507 (1977).

[36]A. Gupta, D. S. Perry, and R. N. Zare, J. Chem. Phys. **72**, 6250 (1980).

[37]Considerations similar to those applied here to the reactions with N_2O may help explain other discrepancies noted in Ref. 9. In particular, CO_2 does not correlate with ground state CO and O but with $O(^1D)$.

[38]The *ab initio* calculations of Ref. 16(b) show 0.57 electrons transferred from Ni to O in the NiO ground state.

[39]C. Lifshitz, R. L. C. Wu, T. O. Tiernan, and D. T. Terwilliger, J. Chem. Phys. **68**, 247 (1978).